Effects of triphenyltin on glycinergic transmission on rat spinal neurons

Kazuki Noma [a], Hironari Akaike [a], Yuki Kurauchi [a], Hiroshi Katsuki [a],

Yasuo Oyama [b], Norio Akaike [a,c,d]

[a] Graduate School of Pharmaceutical Sciences, Kumamoto University, 5-1 Oe-Honmachi, Chuo-ku, Kumamoto 862-0973, Japan

[b] Laboratory of Bioassessment, Faculty of Bioscience and Bioindustry, Tokushima University, Minami-Josanjima 2-1, Tokushima 770-8501, Japan

[c] Research Division for Clinical Pharmacology, Medical Corporation, Juryo Group, Kumamoto Kinoh Hospital, 6-8-1 Yamamuro, Kita-ku, Kumamoto 860-8518, Japan

[d] Research Division of Neurophysiology, Kitamoto Hospital, 3-7-6 Kawarasone, Koshigaya, Saitama 343-0821, Japan

Running title: Triphenyltin and glycinergic transmission

Key words: Triphenyltin; Environmental pollution; Spinal neuron; Synaptic bouton preparation; Glycinergic transmission

Abstract

Glycine is a fast inhibitory transmitter like γ-aminobutyric acid in the mammalian spinal cord and brainstem, and it is involved in motor reflex, nociception, and neuronal development. Triphenyltin (TPT) is an organometallic compound causing environmental hazard to many wild creatures. Our previous findings show that TPT ultimately induces a drain and/or exhaustion of glutamate in excitatory presynaptic nerve terminals, resulted in blockage of neurotransmission as well as methylmercury. Therefore, we have investigated the neurotoxic mechanism how TPT modulates inhibitory glycinergic transmission in the synaptic bouton preparation of rat isolated spinal neurons using a patch clamp technique. TPT at environmentally relevant concentrations (3–300 nM) significantly increased the number of frequency of glycinergic spontaneous and miniature inhibitory postsynaptic currents (sIPSC and mIPSC) without affecting the current amplitude and decay time. The TPT effects were also observed in external Ca^{2+}-free solution containing tetrodotoxin (TTX) but removed in Ca^{2+}-free solution with both TTX and BAPTA-AM (Ca^{2+} chelator). On the other hand, the amplitude of glycinergic evoked inhibitory postsynaptic currents (eIPSCs) increased with decreasing failure rate (Rf) and paired pulse ratio (PPR) in the presence of 300 nM TPT. At a high concentration (1 μM), TPT completely blocked eIPSCs after a transient facilitation. Overall, these results suggest that TPT directly acts transmitter-releasing machinery in glycinergic nerve terminals. Effects of TPT on the nerve terminals releasing fast transmitters were greater in the order of glycinergic > glutamatergic > GABAergic ones. Thus, TPT is supposed to cause a strong synaptic modulations on glycinergic neurotransmission in wild creatures.

Keywords: triphenyltin; glycine; neuronal transmission; postsynaptic current

Highlights

- Effects of triphenyltin (TPT) were examined using ‘synaptic bouton’ preparation.
- TPT did not change extrasynaptic glycine receptor-mediated responses.
- TPT modulated glycinergic spontaneous and evoked synaptic responses.
- TPT at high concentrations finally depleted glycine in the nerve terminal.
- It is likely that TPT causes breaking down of neuronal excitability in wild creatures.

1. Introduction

Triphenyltin (TPT) has been applied as a biocide for agricultural and industrial purposes such as fungicide and antifoulant, respectively (Yi et al., 2012). Even though the use of TPT has been prohibited, some of farmers illegally used this compound as a fungicide (Wu et al., 2010). Increasing trend of pollution of TPT as an antifoulant was also reported in coasts of Taiwan (Meng et al., 2005) and Hong Kong (Ho and Leung, 2014). Because health impacts of TPT are still concerned in these countries, the risk assessment of intake of organotin compounds from fish and seafood has been conducted in Taiwanese population (Lee et al., 2016). Levels of phenyltins in fish and seafood are higher than those of butyltins (Lee et al., 2016). TPT is supposed to be less neurotoxic than trialkyltins (Snoeij et al., 1985; Besser et al., 1987). However, diplopia, drowsiness, giddiness, vertigo, bidirectional nystagmus, impairment of calculation ability, as well as disorientation to time, people and place were developed without significant findings by magnetic resonance imaging and single-photon emission computed tomography in TPT poisoning patient (Lin et al., 1998), suggesting a possibility that TPT causes cellular dysfunction of brain without structural damage, which results in variable CNS clinical presentations. In fact, TPT at nanomolar concentrations facilitates voltage-dependent Na^+ current and decreases voltage-dependent K^+ current of rat brain neurons (Oyama and Akaike, 1990). Furthermore, glutamatergic spontaneous and action potential-evoked excitatory postsynaptic currents (sEPSC and eEPSC) in rat hippocampal CA3 neurons were also promoted by TPT at similar concentrations (Wakita et al., 2015). Thus, TPT is considered to be a neurotoxicant.

Neuronal excitability is influenced by relative distribution (balance) of excitatory and inhibitory synaptic inputs. Therefore, it is also important to examine the effects of TPT on inhibitory synaptic transmission in order to reveal the cellular basis of neurotoxic actions of TPT. In this study, we examined the effects of TPT on glycinergic and GABAergic inhibitory

synaptic transmissions using well established ‘synaptic bouton’ preparation (Akaike and Moorhouse, 2003) that allows spontaneous and evoked inhibitory synaptic activities such as spontaneous and evoked inhibitory postsynaptic currents (sIPSC, mIPSC and eIPSC) from isolated brain cells. Glycine is an important fast inhibitory transmitter in vital spinal and supraspinal (brainstem) interneurons of mammalian nervous system, especially in the ventral horn where glycinergic transmission is involved in motor reflex and nociception as well as fast GABAergic transmission (Bowery and Smart, 2006; Harvey et al., 2004). In addition, extrasynaptic (non-synaptic) glycine receptors on nerve cell bodies (soma membrane) are important for neuronal development (Flint et al., 1998) and for tonically active state of neurons by locally released inhibitory substances (Mori et al., 2002). Therefore, it is valuable to study the TPT-induced modulation on the inhibitory glycinergic transmissions (sIPSC and eIPSC) and extrasynaptic glycine receptor-mediated current (I_{Gly}) in mammalian spinal cord. The obtained data are compared GABAergic and glutamatergic ones.

2. Materials and Methods

2.1. Cell preparation – ‘synaptic bouton’ preparation

The use of experimental animals was approved by the Ethics Committee of Kumamoto Kinoh Hospital.

Details of the “synaptic bouton” preparation were described previously (Murakami et al., 2002; Akaike and Moorhouse, 2003). Briefly, Wistar rats (11–23 days old, either sex) were decapitated under pentobarbital (50 mg/kg, i.p.) anesthesia. The brain was removed and immersed in ice-cold oxygenated incubation medium. The ionic composition of the incubation medium is shown in Table 1.

(Table 1 near here)

Spinal cord slices (400 μm thick) were prepared using a vibrating microtome (VR 1200S; Leica, Nussloch, Germany). The tip of the glass pipette coupled to a vibration device (S1-10 Cell Isolator; K.T. Labs, Tokyo, Japan) was placed on the surface of the slice containing spinal sacral commissural nucleus (SDCN) and was horizontally vibrated at 50 Hz. After mechanical dissociation, the neurons adhered to the bottom of the culture dish.

2.2. Electrophysiological measurements

All recordings were obtained from the 'synaptic bouton' preparation of SDCN neurons receiving multiple inputs from many boutons using conventional whole-cell patch-clamp recordings in voltage-clamp mode. Glycinergic spontaneous, miniature and action potential-evoked inhibitory postsynaptic currents (sIPSCs, mIPSCs, eIPSCs), and glycine or GABA receptor-mediated extrasynaptic currents (I_{Gly} or I_{GABA}) were recorded at a holding potential (V_H) of 0 mV. Extrasynaptic glutamate response (I_{Glu}) and NMDA response (I_{NMDA}) were recorded at a V_H of –65 mV and –40 mV, respectively. All experiments were performed at room temperature (21–24 ºC). The resistances of the recording pipettes filled with the internal solution were 3–6 MΩ. All membrane currents were acquired with 20 kHz sampling rate and stored on a computer using pCLAMP 10.2 (Axon Instruments, CA, USA). Compositions of external and internal pipette solutions for recording the receptor-activated currents are listed in Table 2. Voltage-dependent Na^+ channel currents (I_{Na}) and Ba^{2+}-permeable high-threshold Ca^{2+} channel currents (I_{Ba}) were recorded at V_H of −70 mV and −60 mV, respectively. The solutions for recording voltage-gated currents are shown in Table 3.

(Tables 2 and 3 near here)

2.3. Paired-pulse focal electrical stimulation of single boutons using glass pipettes

Focal electrical stimulation of a single bouton adherent to dissociated CNS neurons has been described previously (Akaike and Moorhouse, 2003). Focal electric stimuli using a bipolar

pipette (theta glass) were employed to activate a single glycinergic nerve terminal synapsing an isolated SDCN neuron to measure eIPSCs. Stimulus shocks were delivered for 100 μs at intensities of 0.06–0.1 mA with inter-stimulus intervals of 40 ms for glycinergic eIPSCs. The stimulating electrode was moved along the surface membrane of SDCN neuron but did not directly touch the membrane of a bouton. Periodic shocks were delivered while monitoring whole-cell currents until eIPSCs appeared. Membrane resistance was not changed during the application of TPT because the base-line of current was not changed.

2.4. Drugs and application

TPT was distributed by Tokyo Chemical Industry Co., Ltd. (Tokyo, Japan). TPT was initially dissolved in dimethyl sulfoxide (DMSO) and the TPT solution (10–1000 μM) was then added to the external solution to achieve final concentrations (10–1000 nM) of TPT. DMSO at 0.1 % did not affect electrophysiological parameters examined in this study. Reagents to prepare the solutions listed in Tables 2 and 3 were obtained from Wako Pure Chemicals (Osaka, Japan) and Sigma-Aldrich (St. Louis, MO, USA). Tetrodotoxin (TTX) was obtained from Sigma-Aldrich. All test solutions containing drugs were applied using a 'Y-tube system,' which allowed solution exchange around the cells within about 20 ms (Murase et al., 1990). The removal of drug(s) was achieved by switching the external solution containing drug(s) to control solution.

2.5. Data analysis

Currents were analyzed using pCLAMP 10.2 (Axon Instrument). Evoked glycinergic eIPSCs were counted and analyzed in pre-set epochs before, during, and after each test condition. The amplitude, failure rate (Rf) and paired-pulse ratio (PPR) of eIPSCs were analyzed. PPR was calculated by dividing the mean peak amplitude of P_2 by the mean peak amplitude of P_1. The effects of TPT were normalized as relative changes with respect to their

respective controls. Mean amplitude was calculated from all current responses including current amplitude = 0 (full failure). Mean values were obtained under the condition that the amplitude was zero in the case of full failure. In each experiment, glycinergic sIPSCs and mIPSCs, GABAergic sIPSC and glutamatergic sEPSC were counted and analyzed in pre-set epochs before, during, and after each test condition using the MiniAnalysis Program (Synaptosoft, NJ, USA). All Data were analyzed using Origin Pro 7.5 software (OriginLab Corporation, Northampton, MA, USA). Data are reported as means ± S.E.M. of normalized values. Data were tested using one-way ANOVA followed by a post hoc Bonferroni test for multiple comparisons, using absolute values rather than normalized ones. Two-tailed P values of less than 0.05 were considered statistically significant.

3. Results

3.1. Effects of TPT on extrasynaptic glycine, GABA and glutamate receptor-mediated currents (I_{Gly}, I_{GABA} and I_{Glu})

In the present study, exogenous bath application of glycine induced outward currents in synaptic bouton preparation of isolated SDCN neurons at a holding potential (V_H) of 0mV, which is close to glutamatergic reversal potential. The strychnine-sensitive glycine response (I_{Gly}) increased in a concentration-dependent manner (Fig. 1A). In the concentration-response curve of I_{Gly}, 30 μM glycine-induced I_{Gly} showed a little desensitization as shown in Fig. 1A inset (middle). Thus, the effects of TPT at various concentrations (30, 100, 300 and 1000 nM) were tested on 30 μM glycine-induced I_{Gly}. As seen in Fig. 1Ba, TPT at various concentrations had no effects on I_{Gly} (n=4). Current traces of Fig. 1Ba inset show the effect of 300 nM TPT on 30 μM glycine response. Similarly, 30 μM glutamate-, 100 μM NMDA- and 10 μM GABA-receptor mediated responses (I_{Glu}, I_{NMDA} and I_{GABA}) were not affected by application of 300 nM

TPT (Fig. 1Bb–d). I_{GABA} was recorded at a V_H of 0 mV while I_{Glu} and I_{NMDA} at V_H of –65 mV and –40 mV, respectively. Here, NMDA response was elicited in the continuous presence of 1 μM glycine where the glycine receptor existing on NMDA receptor is strychnine-insensitive (DeFeudis et al., 1978). These results clearly indicate that TPT does not disturb the extrasynaptic glycine, GABA, glutamate and NMDA receptors on postsynaptic soma membrane.

(Fig. 1 near here)

3.2. Effects of TPT on glycinergic spontaneous IPSCs (sIPSCs)

Glycinergic sIPSCs were recorded at a V_H of 0mV. The number of frequency of sIPSCs significantly increased in a concentration-dependent fashion when TPT concentration was stepwisely rose from 30 to 100 nM and then to 300 nM (Fig. 2A). 300 nM TPT induced a marked increase of sIPSC frequency after 2–3 min of the application but after that the increased frequency was gradually decreased. The inhibition was not recovered even after removal of TPT. Fig. 2 Ba–c show representative cumulative probabilities for inter-event interval (frequency), amplitude and decay time measured at 1/e from each current peak of sIPSCs under control (solid lines) and with 300 nM TPT (dashed lines). Both the current amplitude and 1/e decay time of sIPSCs were not affected at all by 300 nM TPT. These statistical analyses are summarized in Fig. 2Ca-c.

(Fig. 2 near here)

3.3. Effects of TPT on glycinergic miniature IPSCs (mIPSCs)

To avoid the contribution of Na^+ influxes through voltage-dependent Na^+ channels and/or steady Na^+ inward currents (Yamada-Hanff and Bean, 2013) existing possibly on nerve endings to sIPSCs, tetrodotoxin (TTX), a specific Na^+ channel blocker, was used. In the presence of 300 nM TTX at which concentration TTX completely blocks Na^+ channels (Wakita et al., 2015),

glycinergic spontaneous miniature IPSCs (mIPSCs) were recorded. The mIPSCs showed less frequency as compared with the control (sIPSCs) measured in external solution without TTX. However, TTX did not affect the current amplitude and 1/e decay time of mIPSCs (Fig. 3Aa–b). In this experimental condition, the application of 300nM TPT markedly increased the number of frequency in mIPSC without affecting the amplitude (Fig. 3Ac). Fig. 3B summarized the effects of 300nM TPT on relative frequency (a), relative amplitude (b) and 1/e decay time (ms) (c) of glycinergic mIPSCs (n=4).

(Fig. 3 near here)

Intra-axonal free Ca^{2+} concentration is also regulated by Ca^{2+} influxes through voltage-dependent Ca^{2+} channels triggered by Na^{+} spikes in nerve endings. Therefore, following experiments were performed in Ca^{2+}-free external solution (Ca^{2+}-free solution) containing 300 nM TTX. The number of mIPSC frequency was markedly decreased by application of Ca^{2+}-free solution containing TTX. The amplitude of mIPSC was also decreased significantly (Fig. 4Aa-c). In this experimental condition, 300nM TPT also significantly increased the mIPSCs frequency without affecting the amplitude and 1/e current decay time. All results are summarized in Fig. 4B (n=5).

(Fig. 4 near here)

TPT itself rises the intracellular Ca^{2+} concentration of rat cerebellar neuron even in Ca^{2+}-free external solution (Oyama et al., 1992). Therefore, the effects of 300 nM TPT was examined in synaptic bouton preparation immersed in Ca^{2+}-free solution containing both 300 nM TTX and 30 μM BAPTA-AM, a membrane permeable specific Ca^{2+} chelator. Here, BAPTA-AM was dissolved in DMSO, and the preparation was first pretreated in 1% DMSO Ca^{2+}-free solution for 10 min. As seen in Fig. 5Bc, the 1/e decay time slightly prolonged in Ca^{2+}-free solution containing 1% DMSO. Expectedly, the successive addition of 300 nM TPT did not affect on the frequency, amplitude and 1/e decay time of mIPSC (Fig. 5B).

(Fig. 5 near here)

3.4. Effects of repetitive TPT applications on glycinergic sIPSC

Oyama et al. (1992) showed that TPT directly increases intracellular Ca^{2+} concentration of brain cell. In the present study TPT had no effect on mIPSC frequency in the presence of BAPTA-AM. The results suggest that the increase of intra-axonal Ca^{2+} concentration triggers the increase in glycinergic sIPSC frequency. However, as seen in Figs. 2-4, without BAPTA, TPT at higher concentrations than 300 nM transiently increased the frequency of both sIPSC and mIPSC. Such marked transient facilitation of sIPSC frequency by 1st application of 300 and 1000 nM disappeared at the 2nd application (Fig. 6A and B). Especially, 2nd application of 1000 nM TPT increased little the sIPSC frequency, and then appearance of sIPSC almost ceased and never recovered, suggesting depletion of Ca^{2+} release from Ca^{2+} stores.

(Fig. 6 near here)

3.5. Effects of TPT on action potential-evoked glycinergic inhibitory postsynaptic currents (eIPSCs)

Fig. 7A shows typical time course of outwardly-directed fast glycinergic inhibitory postsynaptic currents (eIPSCs) in response to focal paired-pulse stimulation (40 ms interval) with and without 300 nM TPT. Focal stimulation produced glycinergic eIPSCs in response to both the first (P_1) and second (P_2) stimuli with occasional failures. When TPT was applied for 5 min, TPT gradually potentiated P_1 and P_2 current amplitude with decreasing both PPR and Rf where PPR is P_2/P_1 amplitude ratio (paired-pulse current ratio) and Rf is failure rate. The mean value of P_1 amplitude, Rf and PPR of eIPSCs in the presence of 300 nM TPT are summarized in Ac (n = 5). Effects of 300 nM TPT on eIPSC were recovered somewhat incompletely followed by Rf increase by washing out the drug (Fig. 7Aa, b). 1/e decay time values with and without 300 nM TPT were 9.0 ± 0.25 ms (n = 16 events) and 9.6 ± 0.49 ms (n = 32 events), respectively.

As shown in Fig. 6B, TPT of higher concentration (1000 nM) transiently increased the

frequency of sIPSCs and then the increased frequency decreased gradually. Finally the sIPSCs ceased completely. Similarly, 1000 nM TPT also increased transiently the P_1 amplitude of eIPSC with decreasing Rf and PPR but after that eIPSC disappeared during application of TPT and never recovered washing out TPT (Fig. 7Ba, b).

(Fig. 7 near here)

3.6. Effects of TPT on GABAergic and glutamatergic spontaneous postsynaptic currents (sIPSCs and sEPSCs)

TPT was applied stepwisely at concentration range from 30 to 1000 nM for GABAergic sIPSCs and from 30 to 300 nM for glutamatergic sEPSCs. TPT had little effects on the frequency of GABAergic sIPSCs at concentrations less than 300 nM, but the significant increase of sIPSC frequency appeared at a high concentration of 1000 nM. TPT had no effects on both the amplitude and 1/e decay time (Fig. 8A–C).

Figure 9 shows the effects of TPT on glutamatergic sEPSCs. Effects of TPT on sEPSC frequency significantly appeared at 300 nM without affecting the amplitude and 1/e decay time. The results were summarized in Fig. 9C. All data was obtained from 4 neurons.

(Figs. 8 and 9 near here)

3.7. Effects of TPT on voltage-dependent Na^+ and Ca^{2+} channel currents

As shown in Fig. 10A, TPT at 300 nM did not affect voltage-dependent Na^+ current (I_{Na}) elicited by a depolarization to -20 mV from a holding potential of -70 mV. TPT also exerted no action on voltage-dependent Ba^{2+} current (I_{Ba}) through Ca^{2+} channels activated by a depolarization to 0 mV from a holding potential of -60 mV. Thus, it is evident that TPT at 300 nM has no effects on both I_{Na} and I_{Ba} of rat spinal neurons.

(Fig. 10 near here)

4. Discussion

4.1. TPT action on extrasynaptic receptors

There are strychinine-sensitive and -insensitive glycine receptors (Lynch, 2004; Schmieden et al., 1996). In the present study, both strychinine-sensitive extrasynaptic glycine receptor-gated Cl^- current and cation current elicited by NMDA receptor coexisting with strychinine-insensitive glycine receptor were not affected by TPT. TPT also had no effect on extrasynaptic glutamate and GABA receptor-mediated currents. The results clearly indicate that TPT does not act on these excitatory on inhibitory extrasynaptic receptors on nerve cell body. Thus, it is unlikely that TPT exerts direct actions on signal receptions mediated by neurotransmitters.

4.2. Possible site of TPT action at neuronal synaptic transmissions

The frequency of glycinergic and GABAergic sIPSCs and glutamatergic sEPSCs was strongly increased, in the order of glycinergic, glutamatergic and GABAergic ones, by adding 300 nM TPT: i.g. sensitivity of glycinergic sIPSCs for TPT is 10 times higher than that of GABAergic sIPSCs. Furthermore, the increase of glycinergic sIPSC frequency at 300nM TPT appeared even in Ca-free external solution containing TTX but completely disappeared in Ca-free external solution in the presence of TTX and BAPTA-AM. The results indicate that TPT directly acts on transmitter release machinery in presynaptic nerve endings. TPT is supposed to facilitate the glycinergic synaptic transmission via its action on intracellular calcium store site. However TPT of high concentration causes the depletion of glycine release via intracellular free Ca^{2+}. Therefore these results may also suggest that TPT actions depending on intracellular TPT accumulation causes complicated poisoning symptom in wild creatures. TPT is lipophilic (log[Kow] = 4.19) and membrane-permeable. Therefore, TPT is supposed to affect membranes and intracellular organella. It may be unlikely that TPT is transformed by the cells

because TPT is accumulated in wild creatures.

4.3. Effects of TPT on ionic channels

300 nM TPT increased the frequency of glycinergic sIPSC at $p < 0.001$ without changing the amplitude and 1/e decay time (see Fig. 2). Since glycine release from glycinergic nerve terminal depends on rise of intra-axonal Ca^{2+} concentration, one of possible mechanisms of glycine release seems to be involvement of TPT on voltage-dependent ionic channels (Na^+, Ca^{2+} and K^+ channels) in nerve ending that trigger Ca influxes directly and/or indirectly. Oyama and Akaike (1990) found that 300 nM TPT in the cell body of rat hippocampal CA1 neurons inhibited partially the peak current and prolonged the decay time of voltage-dependent Na^+ current (I_{Na}), and that TPT inhibited 10% of delayed K^+ current (I_{KD}) and 40% of transient K^+ current (I_A). Wakita et al., (2015) also reported that 300 nM TPT slightly inhibited I_{Na} but had no effect on high-threshold Ca^{2+} channels (I_{Ca}) in rat hippocampal CA3 neurons. According to our previous papers, the functional distribution of Ca^{2+} channel subtypes in GABAergic (Murakami et al., 2002), glycinergic (Nonaka et al., unpublished data) and glutamatergic (Shin et al., 2011) nerve terminals synapsing rat hippocampal CA1 neuron, spinal sensory neuron and hippocampal CA3 neuron was almost similar to that on their postsynaptic soma membrane, even through there are more or less differences in density of distribution among their subtypes. In the present SDCN neurons, however, 300 nM TPT did not inhibit both I_{Na} and I_{Ba} (Fig. 10). In addition 300 nM TPT could increase the frequency of glycinergic mIPSCs measured in Ca^{2+}-free external solution containing 300 nM TTX. Therefore, all over the results suggest that contribution of 300 nM TPT on voltage-dependent ionic channels on glycinergic nerve terminal is almost negligible, and that TPT directly acts to glycinergic nerve endings.

4.4. TPT-induced disturbance of neuronal integration

Glycine receptors mediate fast synaptic inhibition as well as GABA in the spinal cord of the mammalian central nervous system (CNS) that controls sensory and motor functions (Legendre, 2001). Binding of glycine to its postsynaptic receptor leads to the increase in membrane Cl^- permeability that hyperpolarizes post-synaptic membranes, depending on Cl^- equilibrium potential (Young and Snyder, 1973). Thus, the hyperpolarization reduces neuronal excitability by attenuating generation of action potentials. Glycine receptors are found at intra- and extra-synaptic regions of cell body in spinal neurons. As to sensory function, the activation of glycine receptors attenuates the transmission of nociceptive signals to higher brain regions. This process contributes pain sensitization mediated by inflammatory mediators such as prostaglandins (Harvey et al., 2004). Concerning motor function, the activation of glycine receptors is proposed to dampen brainstem and spinal reflexes that involve the somatic motor system (Bolon et al., 2013).

In the present study, TPT hardly affected extrasynaptic inhibitory strychnine-sensitive glycine response (I_{Gly}) and GABA response (I_{GABA}). Also, TPT had no effects on excitatory extrasynaptic glutamate response (I_{Glu}) and NMDA response (I_{NMDA}) being governed by strychnine-insensitive glycine receptor. The results indicate that TPT does not directly modulate on these excitatory and inhibitory extrasynaptic receptors on nerve cell body.

The treatment with TPT is supposed to induce complex modifications of glycinergic synaptic transmission, depending on the concentrations of TPT. TPT at lower concentrations facilitated synaptic transmission by increasing glycine release from presynaptic terminals. TPT at higher concentration transiently induced further facilitation of synaptic transmission during TPT application and thereafter inhibited the glycinergic transmission. The phenomena caused by TPT were similarly observed under external Ca^{2+}-free external solution with TTX. TPT increased intracellular Ca^{2+} concentration under external Ca^{2+}-free conditions in rat cerebellar neurons (Oyama et al., 1992). In the present study, facilitatory actions of TPT on mIPSC frequency completely disappeared in Ca^{2+}-free external solution with TTX containing

BAPTA-AM. Thus, it is likely that TPT increases the intracellular Ca^{2+} concentration and that TPT releases glycine from synaptic terminal without membrane depolarization and Ca^{2+} influx. The increase in intracellular Ca^{2+} concentration of nerve endings by TPT is supposed to be linked to the release of glycine. It is known that Ca^{2+}-triggered fusion of synaptic vesicles and neurotransmitter release are fundamental signaling steps (Schneggenburger and Neher, 2000). It is generally recognized that fast transmitter release is triggered by elevations in intracellular Ca^{2+} concentration near the sites of vesicle fusion. Therefore, it is likely that excessive elevation of intracellular Ca^{2+} level by TPT finally causes non-reversible change in transmitter release mechanisms, resulting in loss of functional roles in nerve terminal.

It is difficult to precisely predict the influence of TPT on nervous system only from the TPT actions on glycinergic transmission because TPT seems to exert similar actions on neuronal transmission mediated by glutamate in hippocampus (Wakita et al., 2015) and by GABA (present study). The nervous system in spinal cord has three basic functions such as sensory input, integration of input and motor output. Glycinergic transmission at spinal cord is involved in both sensory input and motor outputs. From the results of previous and present studies, it is considered that environmentally-relevant concentrations of TPT promote more or less both excitatory and inhibitory neuronal transmissions. Therefore, relative distribution of excitatory and inhibitory synaptic inputs may determine the excitability (or the balance between excitation and inhibition) of postsynaptic sensory and motor neurons. At present, there are only a few neurophysiological works to investigate how neuronal circuits affect the balance of excitation and inhibition (Dehghani et al., 2016; Okun and Lampl, 2016; Wahlstrom-Helgren and Klyachko, 2016). TPT may disrupt the balance of excitation and inhibition of sensory and motor neurons, resulting in malfunction in the integration of neuronal circuit.

Acknowledgments

This work is supported by Grant-in-Aid from Kumamoto Kinoh Hospital and Grand-in-Aid from Kitamoto Hospital for N. Akaike.

Conflict of interest

No conflicts of interest, financial or otherwise, are declared by the authors.

Author Contributions

N. A. conceived and designed research; K. N., Y. K. and H. A. performed experiments and analyzed data under the direction of H. K.. Y. O. and N. A. edited and drafted manuscript.

References

Akaike, N., Moorhouse, A.J., 2003. Techniques: Applications of the nerve–bouton preparation in neuropharmacology. Trend Pharmacol. Sci. 24(1), 44–47.

Besser, R., Krämer, G., Thümler, R., Bohl, J., Gutmann, L., Hopf, H.C., 1987. Acute trimethyltin limbic-cerebellar syndrome. Neurology 37(6), 945–945.

Bowery, N.G., Smart, T.G., 2006. GABA and glycine as neurotransmitters: a brief history. Brit. J. Pharmacol. 147, S109–S119.

Bolon, B., Butt, M.T., Garman, R.H., Dorman, D.C., 2013. Nervous System in Haschek and Rousseaux's Handbook of Toxicologic Pathology (Third Edition).

DeFeudis, F.V., Muñoz, L.O., Fando, J.L., 1978. High-affinity glycine binding sites in rat CNS: regional variation and strychnine sensitivity. Gen. Pharmacol: Vasc. Syst. 9(3), 171–176.

Dehghani, N., Peyrache, A., Telenczuk, B., Le Van Quyen, M., Halgren, E., Cash, S.S., Hatsopoulos, N.G., Destexhe, A., 2016. Dynamic balance of excitation and inhibition in human and monkey neocortex. Sci. Rep. 6, 23176.

Flint, A. C., Liu, X., Kriegstein, A.R., 1998. Nonsynaptic glycine receptor activation during early neocortical development. Neuron 20, 43–53.

Harvey, R.J., Depner U.B., Wassle, H., Ahmadi, S., Heindl, C., Reinold, H., Smart, T.G., Harvey, K., Schutz, B., Abo-Salem, O.M., Zimmer, A., Poisbeau, P., Welzl, H., Wolber, D.P., Betz, H., Zeihofer, H.U., Muller, U., 2004. GlyR alpha3: an essential target for spinal PGE2-mediated inflammatory pain sensitization. Science 304, 884–887.

Ho, K.K., Leung, K.M., 2014. Organotin contamination in seafood and its implication for human health risk in Hong Kong. Marine Poll. Bull. 85(2), 634–640.

Jang, I.S., Jeong, H.J., Katsurabayashi, S., Akaike, N., 2002. Functional roles of presynaptic GABAA receptors on glycinergic nerve terminals in the rat spinal cord. J. Physiol. 541(2), 423–434.

Lee, C.C., Hsu, Y.C., Kao, Y.T., Chen, H.L., 2016. Health risk assessment of the intake of butyltin and phenyltin compounds from fish and seafood in Taiwanese population. Chemosphere 164, 568–575.

Legendre, P., 2001. The glycinergic inhibitory synapse. Cell. Mol. Life Sci. 58, 760–793.

Lin, T.J., Hung, D.Z., Kao, C.H., Hu, W.H., Yang, D.Y., 1998. Unique cerebral dysfunction following triphenyltin acetate poisoning. Human Exp. Toxicol., 17(7), 403–405.

Lynch, J.W., 2004. Molecular structure and function of the glycine receptor chloride channel. Physiol. Rev., 84, 1051–2004.

Meng, P.J., Wang, J.T., Liu, L.L., Chen, M.H., Hung, T.C., 2005. Toxicity and bioaccumulation of tributyltin and triphenyltin on oysters and rock shells collected from Taiwan mariculture area. Sci. Total Environ. 349, 140–149.

Mori, M. Gahwiler, B.H., Gerber, U., 2002. Beta-alanine and taurine as endogenous agonists at glycine receptors in rat hippocampus in vitro. J. Physiol., 539, 191–200.

Murakami, N., Ishibashi, H., Katsurabayashi, S., Akaike, N., 2002. Calcium channel subtypes on single GABAergic presynaptic terminal projecting to rat hippocampal neurons. Brain Res. 951(1), 121–129.

Murase, K., Ryu, P.D., Randic, M., 1989. Excitatory and inhibitory amino acids and peptide-induced responses in acutely isolated rat spinal dorsal horn neurons. Neurosci. Lett. 103, 56–63.

Okun, M., Lampl, I., 2016. Balance of Excitation and Inhibition. In Scholarpedia of Touch (pp. 577-590). Atlantis Press.

Oyama, Y., Akaike, N., 1990. Triphenyltin: a potent excitatory neurotoxicant. Its reciprocal effects on voltage-dependent Na and K currents of mammalian brain neuron. Neurosci. Lett. 119(2), 261–264.

Oyama, Y., Chikahisa, L., Hayashi, A., Ueha, T., Sato, M., Matoba, H., 1992. Triphenyltin-induced increase in the intracellular Ca^{2+} of dissociated mammalian CNS

neuron: its independence from voltage-dependent Ca^{2+} channels. Jpn. J. Pharmacol. 58(4), 467–471.

Schmieden, V., Jezequel, S., Betz, H., 1996. Novel antagonists of the inhibitory glycine receptor derived from quinolinic acid compounds. Mol. Pharmacol. 50, 1200–1206.

Schneggenburger, R., Neher, E., 2000. Intracellular calcium dependence of transmitter release rates at a fast central synapse. Nature 406(6798), 889–893.

Shin, M. C., Wakita, M., Xie, D. J., Iwata, S., Akaike, N., 2011. Synergic effect of diazepam and muscimol via presynaptic GABA A receptors on glutamatergic evoked EPSCs. Brain Res. 1416, 1–9.

Snoeij, N.J., Van Iersel, A.A.J., Penninks, A.H., Seinen, W., 1985. Toxicity of triorganotin compounds: comparative in vivo studies with a series of trialkyltin compounds and triphenyltin chloride in male rats. Toxicol. Appl. Pharmacol. 81(2), 274–286.

Wahlstrom-Helgren, S., Klyachko, V.A., 2016. Dynamic balance of excitation and inhibition rapidly modulates spike probability and precision in feed-forward hippocampal circuits. J. Neurophysiol. 116(6), 2564–2575.

Wakita, M., Nagami, H., Takase, Y., Nakanishi, R., Kotani, N., Akaike, N., 2015. Modifications of excitatory and inhibitory transmission in rat hippocampal pyramidal neurons by acute lithium treatment. Brain Res Bull. 117, 39–44.

Wakita, M., Oyama, Y., Takase, Y., Akaike, N., 2015. Modulation of excitatory synaptic transmission in rat hippocampal CA3 neurons by triphenyltin, an environmental pollutant. Chemosphere 120, 598–607.

Wu, J.Y., Meng, P.J., Liu, M.Y., Chiu, Y.W., Liu, L.L., 2010. A high incidence of imposex in Pomacea apple snails in Taiwan: a decade after triphenyltin was banned. Zoolog. Stud. 49(1), 85–93.

Yamada-Hanff J., Bean, B.P., 2013. Persistent sodium current drives conditional pacemaking in CA1 pyramidal neurons under muscarinic stimulation. J. Neurosci. 33(38), 15011–15021.

Yi, A.X., Leung, K.M., Lam, M.H., Lee, J.S. and Giesy, J.P., 2012. Review of measured concentrations of triphenyltin compounds in marine ecosystems and meta-analysis of their risks to humans and the environment. Chemosphere 89(9), 1015–1025.

Young, A.B., Snyder, S.H., 1973. Strychnine binding associated with glycine receptors of the central nervous system. Proc. Natl. Acad. Sci. USA 70, 2832–2836.

Figures and explanation

Figure 1. The effects of TPT on extrasynaptic glycinergic, glutamatergic (glutamate and NMDA) and GABAergic currents (I_{Gly}, I_{Glu}, I_{NMDA}, I_{GABA}) on postsynaptic soma membrane of SDCN neurons. (A) Dose-response curve of I_{Gly} induced by various glycine concentrations between 3 and 1000 nM. Inset shows typical I_{Gly} elicited by 10, 30 and 100 μM glycine where current desensitization markedly appeared at glycine concentrations higher than 100 μM. V_H = 0mV. (B) a: TPT at 30–1000 nM had no effect on 30 μM glycine-induced outward (I_{Gly}). Current traces in inset show typical I_{Gly} with and without 300 nM TPT. Effects of 30–1000 nM TPT on 30μ M I_{Gly} are shown by filled circles in inset. V_H = 0 mV. b: Effects of 300 nM TPT on 30 μM glutamate-induced inward currents (I_{Glu}). V_H = –65mV. c: Effects of 300 nM TPT on 100 μM NMDA-induced inward current (I_{NMDA}) in the presence of 1 μM glycine. V_H = –40 mV. d: Effects of 300 nM TPT on 10 μM GABA-induced outward currents (I_{GABA}). V_H = 0 mV. Each data of a–d was obtained from 4 neurons. ns, no significant

Figure 2. Effects of TPT at various concentrations on glycinergic spontaneous postsynaptic currents (sIPSCs). (A) TPT was tested in synaptic bouton preparation of isolated SDCN neurons where the drug concentrations were rose stepwisely one after the other from 30 nM to 300 nM. V_H = 0mV. Figure shows representative glycinergic sIPSCs. Stepwise application of TPT increased the frequency of sIPSCs in concentration-dependent manner. w.o., washing out of TPT. Lower expanded current traces are control (left, b) and 300 nM TPT (right, c), obtained from the corresponding time points at upper current trace at slow sweep. (B) Cumulative probabilities of inter-event interval (frequency, a), amplitude (b) and 1/e decay time (c) of sIPSCs recorded under control conditions (solid lines) and the presence of 300 nM TPT (dashed lines). Decay time of current was measured at 1/e point from each peak current (see Bc inset). (C) The effects of TPT at concentrations ranging 30, 100 and 300 nM on the relative frequency

(Freq, a), relative amplitude (Amp, b) and 1/e decay time (ms) (c) of sIPSCs. All events of a and b were normalized to values obtained in the absence of TPT (Cont.). Each value presents mean ± S.E.M. (n = 4–5 neurons). *p < 0.05, **p < 0.001.

Figure 3. Effects of TPT on glycinergic miniature postsynaptic currents (mIPSCs). (A) Representative time course of mIPSC before, during and after adding 300 nM TPT in the presence of 300 nM TTX. Expanded typical current traces a (control, Cont), b (300 nM TTX) and c (300 nM TTX + 300 nM TPT) obtained from the corresponding time points a, b and c in upper panel. (B) Effects of 300 nM TPT on the relative frequency (Freq, a), relative amplitude (Amp, b) and 1/e decay time (ms) (c) of mIPSCc. All events of a and b were normalized to each control value. Histogram shows mean ± S.E.M. from 4 neurons. *p < 0.05; **p < 0.01; ns, no significant

Figure 4. Effects of TPT on glycinergic mIPSCs in Ca^{2+}-free external solution (Ca^{2+} - free). (A) Typical current traces a (Cont), b (Ca^{2+}-free + 300 nM TTX) and c (Ca^{2+}-free + 300 nM TTX + 300 nM TPT) of mIPSCs. (B) Histogram shows relative frequency (Freq, a,), relative amplitude (Amp, b) and 1/e current decay time (ms) (c) of mIPSCs under control condition, Ca^{2+}-free + 300 nM TTX and Ca^{2+}-free + 300 nM TTX + 300 nM TPT. Each value was obtained from 5 neurons. **p < 0.01; ***p < 0.001; ns, no significant

Figure 5. Effects of TPT on mIPSCs in Ca^{2+}-free external solution containing TTX and BAPTA-AM after pretreatment of BAPTA-AM. (A) Representative current traces of sIPSCs of control in normal external solution (a), mIPSCs in Ca^{2+}-free + 300 nM TTX + 30 μM BAPTA (b), and Ca^{2+}-free + 300 nM TTX + 30 μM BAPTA + 300 nM TPT (c). BAPTA was pretreated for 10 min at least. (B) Mean relative frequency (Freq, a), relative amplitude (Amp, b) and 1/e decay time (ms) (c) of sIPSCs and mIPSCs under various experimental conditions. The details

are shown in the bottom of histogram. Data was obtained from 4 neurons. Each value represent mean ± S.E.M. *p < 0.05; ***p < 0.001; ns, no significant.

Figure 6. Effects of repetitive application (2 times) of 300 and 1000 nM TPT on sIPSCs. (A) Typical time course (a) and number of events during 30 s (b) of sIPSCs with 1st and 2nd applications of 300 nM TPT. The sIPSC frequency increased gradually after adding 300 nM TPT and reached the maximal within 3 min. Then the increased frequency recovered to the control level by washing out TPT. However, facilitation of frequency during 2nd TPT application was notably less than the 1st one. (B) 1st application of 1000 nM TPT remarkably increased the sIPSC frequency (a, b), but 2nd application hardly increased the frequency. After that, sIPSCs completely ceased and the recovery was not seen in 4 neurons tested.

Figure 7. Effects of TPT on glycinergic eIPSCs evoked by paired-pulse focal electrical stimuli. (A) Typical eIPSCs before, during and after adding 300 nM TPT. Current traces 1, 2 and 3 in Aa were obtained at time points 1, 2 and 3 in Ab. V_H = 0 mV. Ab shows the representative time course of the peak current amplitude of P_1 (open circle) and P_2 (filled circle) of eIPSC, respectively. Application period of TPT is indicated by a horizontal bar. Ac is relative value of P_1, Rf and PPR (n = 5). Ad is 1/e decay time (ms) of control (16 events) and TPT (32 events). *p < 0.05; ns, no significant (B) eIPSCs before, during and after the addition of 1000 nM TPT. Representative time course of the P_1 peak amplitude (a) and PPR (b) of eIPSCs. Neurons tested in 4 neurons presented similar time courses where all cell responses finally ceased and never recovered.

Figure 8. Effects of TPT at various concentrations on GABAergic spontaneous postsynaptic currents (sIPSCs). (A) GABAergic sIPSCs of control (a) and 1000nM TPT at 3 min after application (b). (B) Effects of 1000 nM TPT on cumulative probabilities of inter-event interval

(a), amplitude (b) and 1/e decay time (c) of GABAergic sIPSCs. (C) Effects of TPT at various concentrations (30–1000 nM) on GABAergic sIPSCs are summarized. a, relative frequency ; b, relative amplitude ; c, 1/e decay time (ms). **$p < 0.01$

Figure 9. Effects of TPT (30–300 nM) on glutamatergic spontaneous postsynaptic currents (sEPSCs). (A) Effects of 300 nM TPT; control (a) and 300nM TPT (b). (B) Effects of 300nM TPT on sEPSCs. Cumulative probabilities of inter-event interval (a), amplitude (b) and 1/e decay time (c). (C) Glutamatergic sEPSCs in the presence of 30–300 nM TPT. Relative frequency (a), relative amplitude (b) and 1/e decay time (ms) (c). All data were obtained from 4 neurons. ***$p < 0.001$

Figure 10. Effects of 300 nM TPT on voltage-dependent ionic currents. (A) Effects of TPT on voltage-dependent Na^+ current (I_{Na}). (B) Effects of TPT on voltage-dependent Ba^{2+} current (I_{Ba}) through Ca^{2+} channels. Data of I_{Na} and I_{Ba} was obtained 5 and 6 neurons, respectively.

Figure 1

Fig. 1

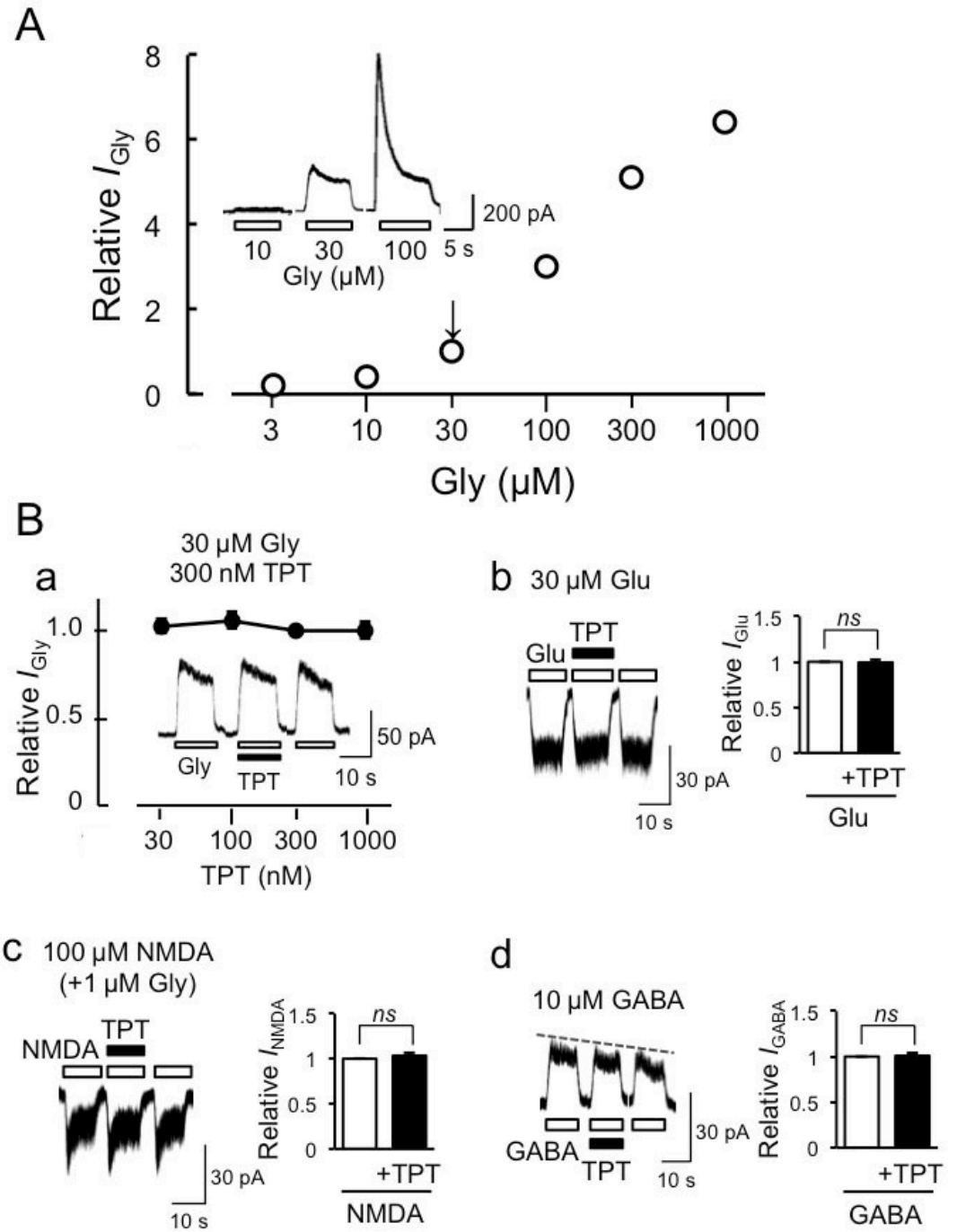

Figure 2

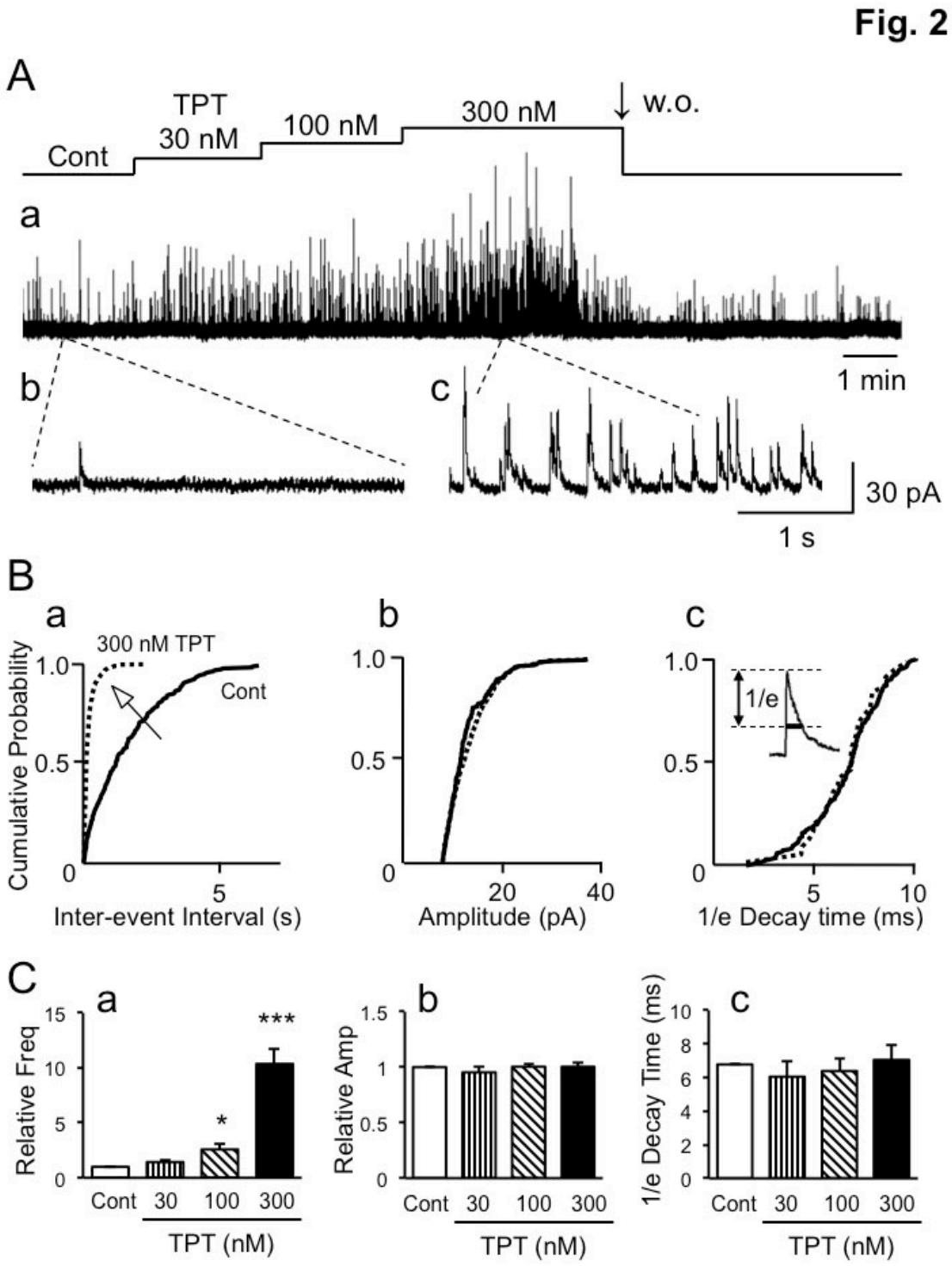
Fig. 2
A
Cont
TPT
30 nM
100 nM
300 nM
w.o.
a
b
c
1 min
30 pA
1 s
B
a
300 nM TPT
Cont
Cumulative Probability
1.0
0.5
0
5
Inter-event Interval (s)
b
1.0
0.5
0
20
40
Amplitude (pA)
c
1/e
1.0
0.5
0
5
10
1/e Decay time (ms)
C
a
Relative Freq
15
10
5
0
***
*
Cont
30
100
300
TPT (nM)
b
Relative Amp
1.5
1
0.5
0
Cont
30
100
300
TPT (nM)
c
1/e Decay Time (ms)
10
8
6
4
2
0
Cont
30
100
300
TPT (nM)

Figure 3

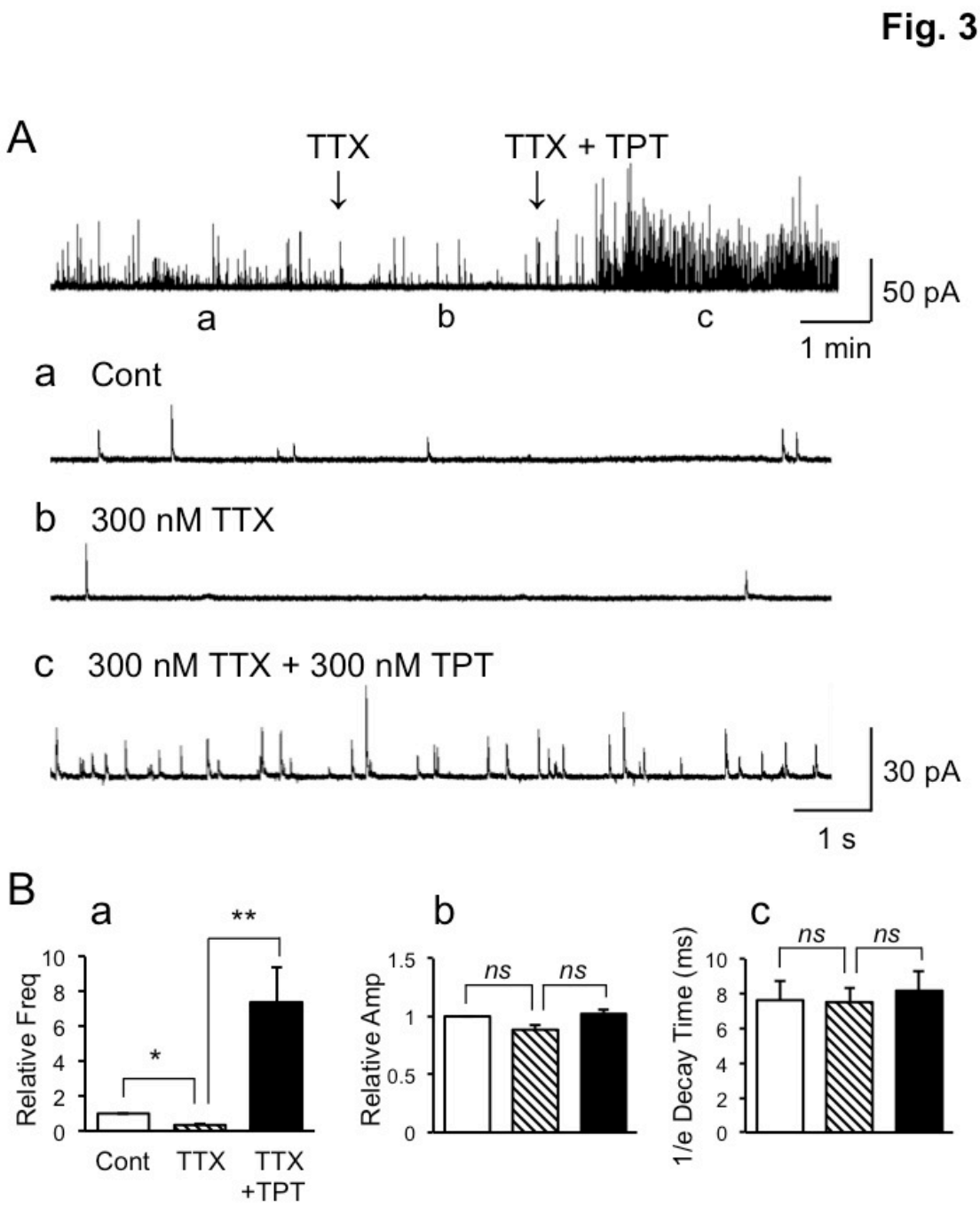
Fig. 3
A
TTX
TTX + TPT
a
b
c
50 pA
1 min
a Cont
b 300 nM TTX
c 300 nM TTX + 300 nM TPT
30 pA
1 s
B
a
Relative Freq
10
8
6
4
2
0
*
**
Cont
TTX
TTX +TPT
b
Relative Amp
1.5
1
0.5
0
ns
ns
c
1/e Decay Time (ms)
10
8
6
4
2
0
ns
ns

Figure 4

Fig. 4

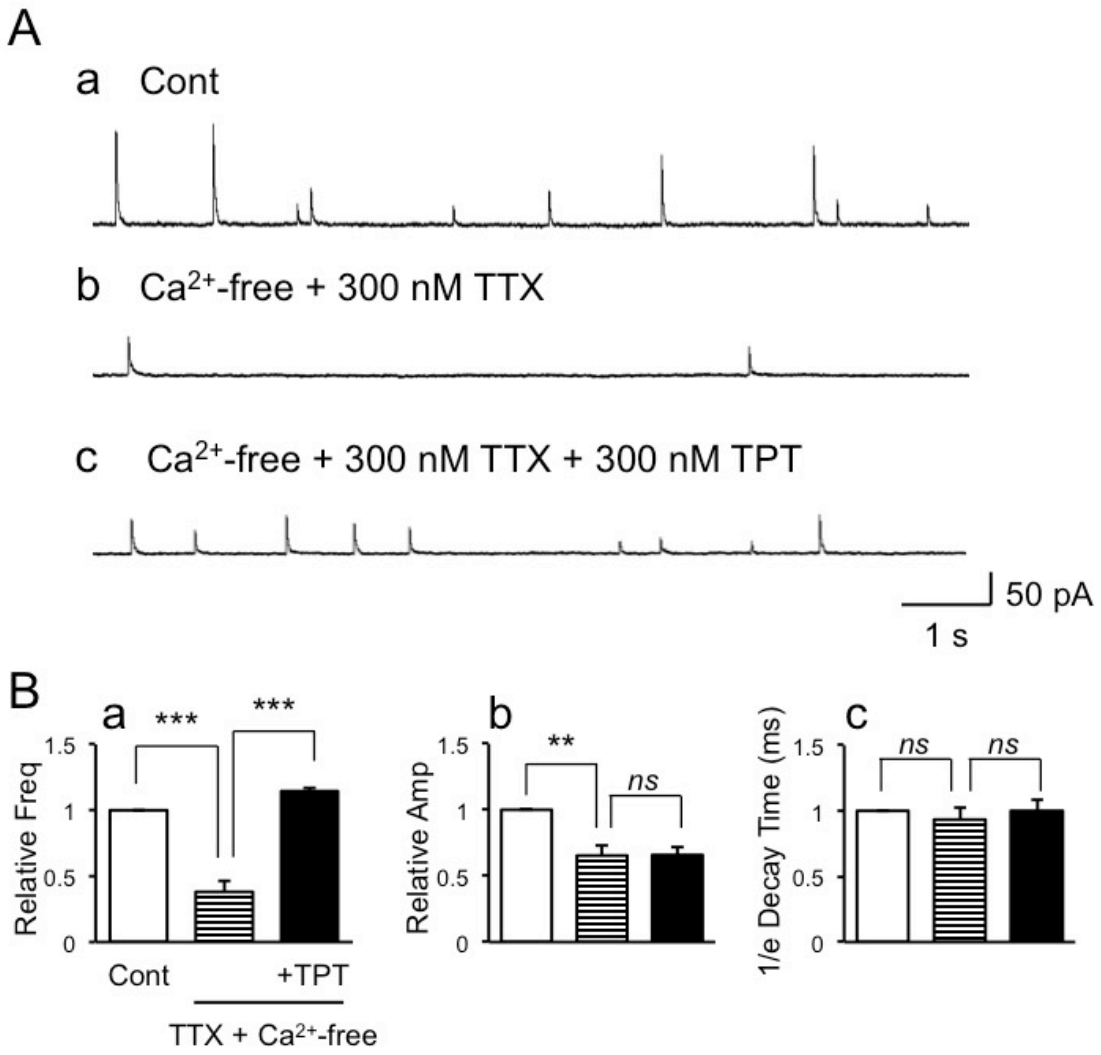

Figure 5

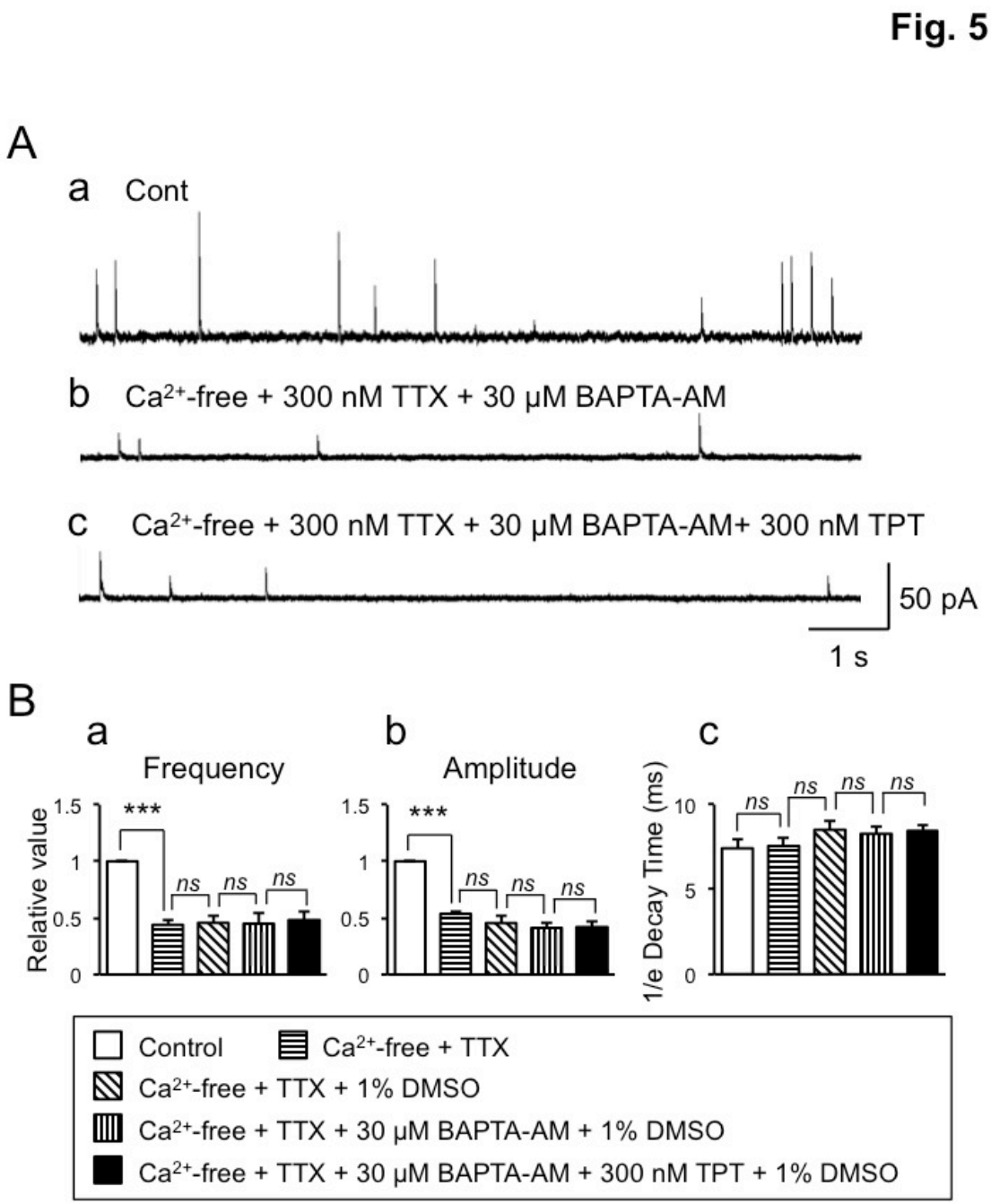
Fig. 5
A
a Cont
b Ca2+-free + 300 nM TTX + 30 μM BAPTA-AM
c Ca2+-free + 300 nM TTX + 30 μM BAPTA-AM+ 300 nM TPT
50 pA
1 s
B
a
Frequency
b
Amplitude
c
Relative value
1/e Decay Time (ms)
***
ns
Control
Ca2+-free + TTX
Ca2+-free + TTX + 1% DMSO
Ca2+-free + TTX + 30 μM BAPTA-AM + 1% DMSO
Ca2+-free + TTX + 30 μM BAPTA-AM + 300 nM TPT + 1% DMSO

Figure 7

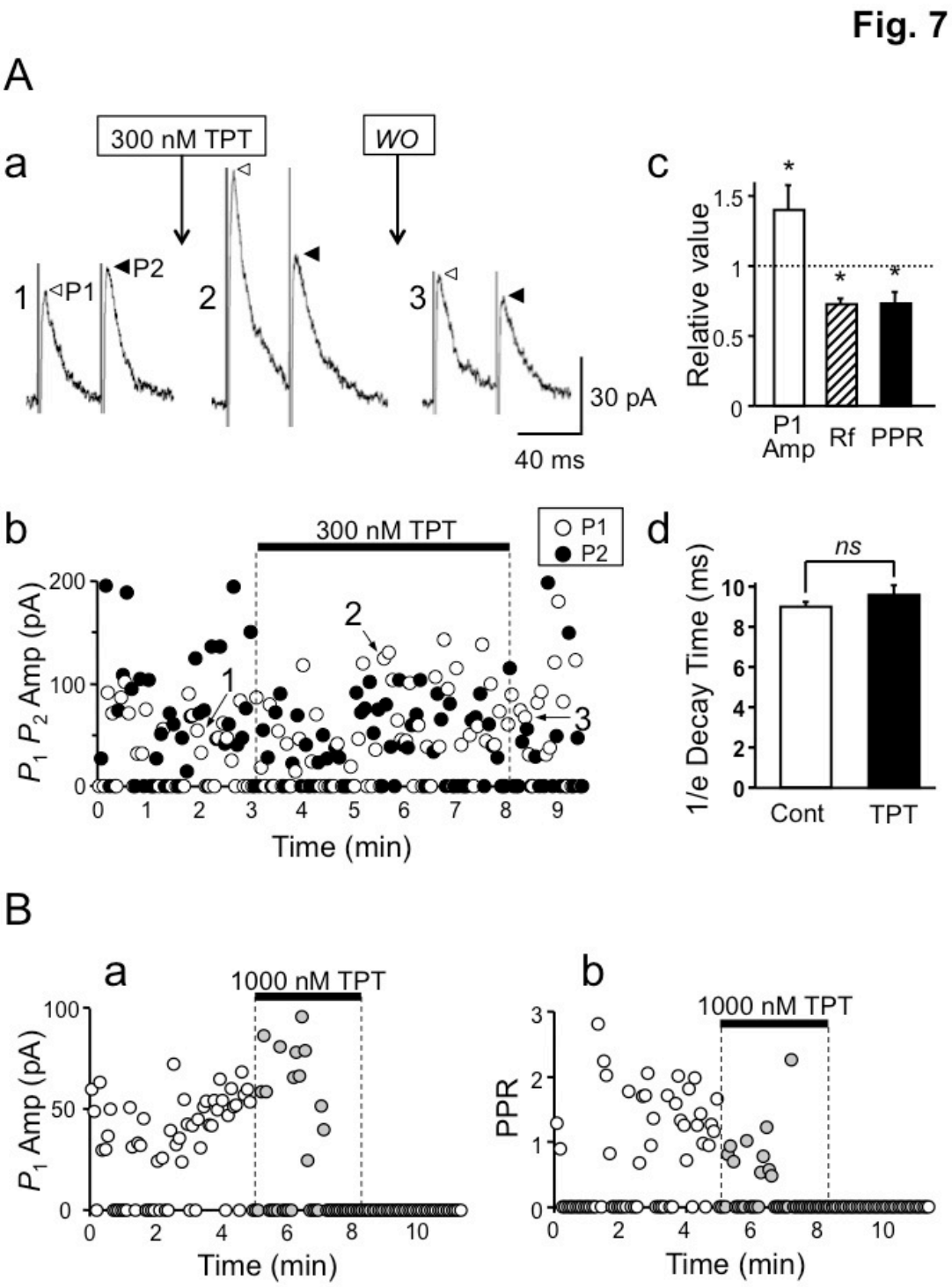
Fig. 7
A
a
300 nM TPT
WO
P1
P2
1
2
3
30 pA
40 ms
c
Relative value
P1 Amp
Rf
PPR
b
300 nM TPT
P1
P2
P1 P2 Amp (pA)
Time (min)
d
ns
1/e Decay Time (ms)
Cont
TPT
B
a
1000 nM TPT
P1 Amp (pA)
Time (min)
b
1000 nM TPT
PPR
Time (min)

Figure 8

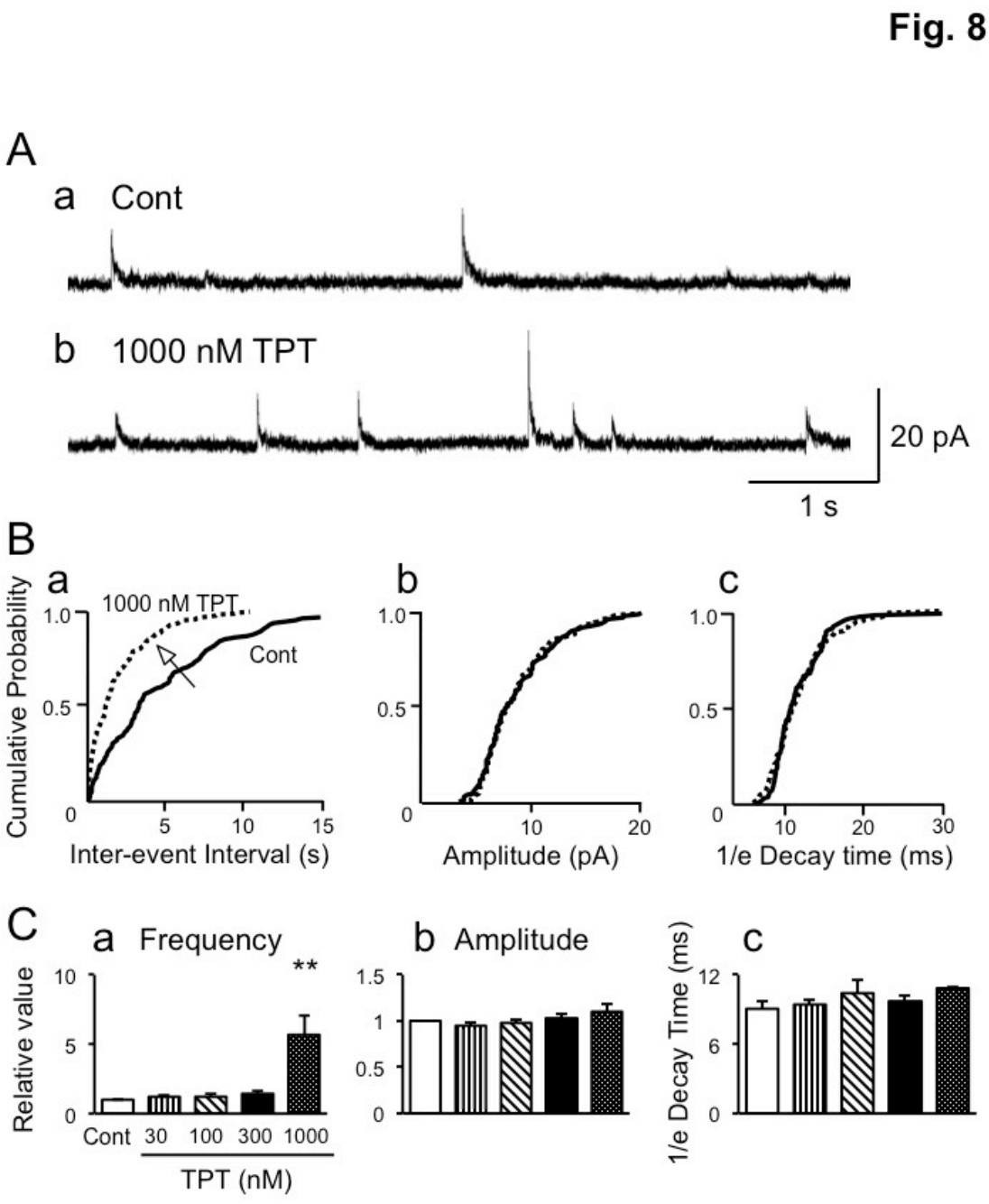
Fig. 8
A
a Cont
b 1000 nM TPT
20 pA
1 s
B
a
1000 nM TPT
Cont
Cumulative Probability
1.0
0.5
0
5
10
15
Inter-event Interval (s)
b
1.0
0.5
0
10
20
Amplitude (pA)
c
1.0
0.5
0
10
20
30
1/e Decay time (ms)
C
a Frequency
**
Relative value
10
5
0
Cont
30
100
300
1000
TPT (nM)
b Amplitude
1.5
1
0.5
0
c
1/e Decay Time (ms)
12
6
0

Figure 9

Fig. 9

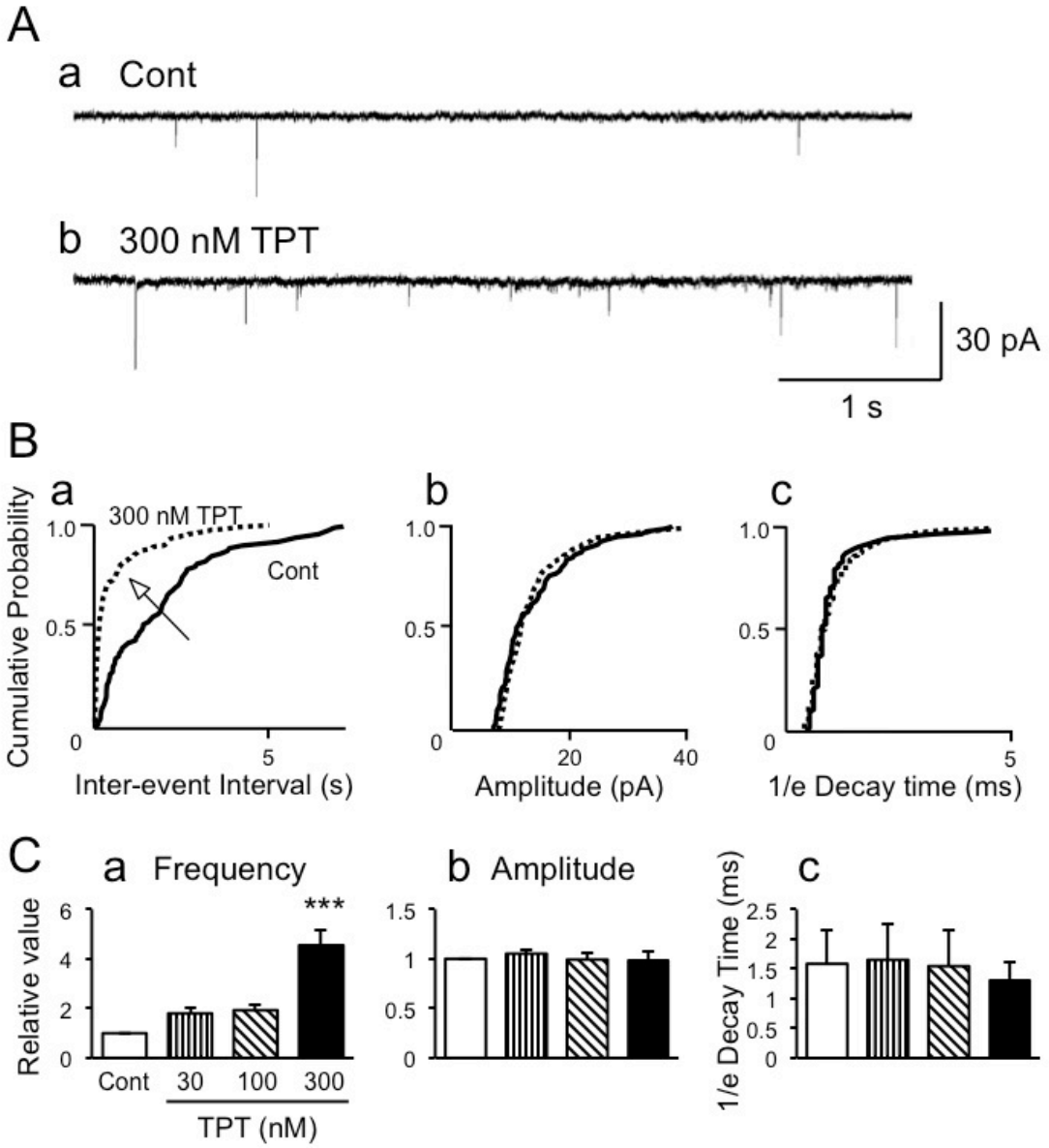

Figure 10

Fig. 10

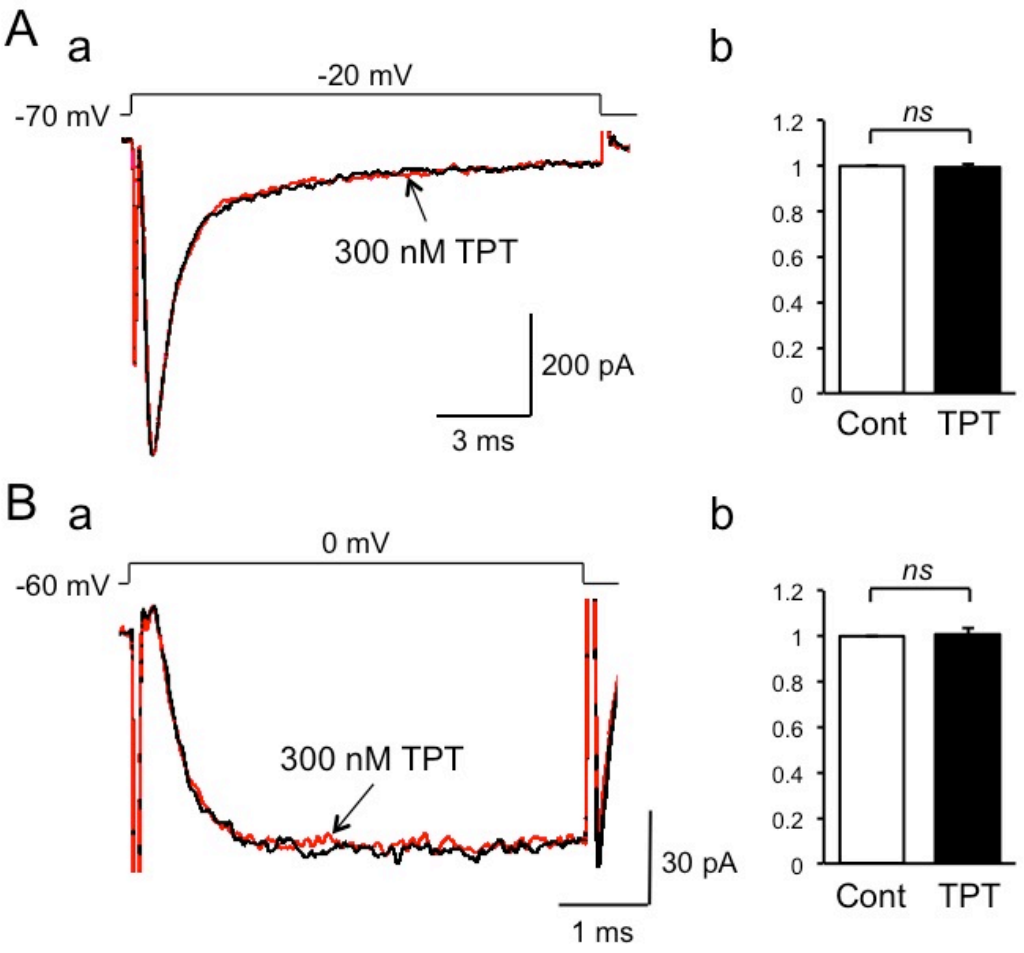

Table 1 Incubation Medium

124 mM NaCl
24 mM $NaHCO_3$
5 mM KCl
1.2 mM KH_2PO_4
2.4 mM $CaCl_2$
1.3 mM $MgSO_4$
10 mM Glucose
Saturated with 95% O_2 and 5% CO_2 to adjust the pH to 7.45

Table 2. Solutions for recording currents elicited by glycine, GABA, and glutamate

Recording Currents	Glycinergic and GABAergic Currents	
	External Solution	Internal Pipette Solution
Composition	150 mM NaCl	5 mM CsCl
	5 mM KCl	135 mM Cs-methanesulfonate
	2 mM $CaCl_2$	5 mM TEA-Cl
	1 mM $MgCl_2$	10 mM EGTA
	10 mM Glucose	10 mM HEPES
	10 mM HEPES	4 mM ATP-Mg
	pH 7.4 Adjusted with Tris base	pH 7.2 Adjusted with Tris base

Recording Current	Glutamatergic Current	
	External Solution	Internal Pipette Solution
Composition	150 mM NaCl	5 mM CsCl
	5 mM KCl	135 mM CsF
	2 mM $CaCl_2$	5 mM TEA-Cl
	1 mM $MgCl_2$	2 mM EGTA
	10 mM Glucose	10 mM HEPES
	10 mM HEPES	5 mM QX-314 bromide
	pH 7.4 Adjusted with Tris base	pH 7.2 Adjusted with Tris base

ATP-Mg; adenosine 5′-triphosphate magnesium salt
EGTA; ethyleneglycol-bis-(α-aminoethylether)-N,N,N′,N′-tetraacetic acid
HEPES; N-2-hydroxyethylpiperazine-N′-2-ethanesulphonic acid
QX-314; 2-((2,6-dimethylphenyl)amino)-N,N,N-triethyl-2-oxoethanaminium
TEA-Cl; tetraethylammonium chloride
Tris base; tris(hydroxymethyl)aminomethane

Table 3. Solutions for recording voltage-dependent currents

Recording Current	Voltage-Dependent Na^+ Current (I_{Na})	
	External Solution	Internal Pipette Solution
Composition	60 mM NaCl	105 mM CsF
	100 mM Choline-Cl	30 mM NaF
	10 mM CsCl	5 mM CsCl
	10 mM glucose	5 mM TEA-Cl
	0.01 mM $LaCl_3$	2 mM EGTA
	5 mM TEA-Cl	10 mM HEPES
	10 mM HEPES	2 mM ATP-Mg
	pH 7.4 Adjusted with Tris base	pH 7.2 Adjusted with Tris base

Recording Current	Ba^{2+} Current (I_{Ba}) Through Voltage-Dependent Ca^{2+} Channels	
	External Solution	Internal Pipette Solution
Composition	145 mM Choline-Cl	80 mM Cs-methanesulfonate
	5 mM CsCl	60 mM CsCl
	5 mM $BaCl_2$	5 mM TEA-Cl
	1 mM $MgCl_2$	2 mM EGTA
	10 mM glucose	10 mM HEPES
	10 mM HEPES	2 mM ATP-Mg
	pH 7.4 Adjusted with Tris base	pH 7.2 Adjusted with Tris base

ATP-Mg; adenosine 5′-triphosphate magnesium salt
EGTA; ethyleneglycol-bis-(α-aminoethylether)-N,N,N′,N′-tetraacetic acid
HEPES; N-2-hydroxyethylpiperazine-N′-2-ethanesulphonic acid
TEA-Cl; tetraethylammonium chloride
Tris base; tris(hydroxymethyl)aminomethane